Microstrip Stepped Impedance Resonator Bandpass Filter With an Extended Optimal Rejection Bandwidth

Jen-Tsai Kuo, *Member, IEEE,* and Eric Shih

***Abstract*—Bandpass filters with an optimal rejection bandwidth are designed using parallel-coupled stepped impedance resonators (SIRs). The fundamental (f_o) and higher order resonant harmonics of an SIR are analyzed against the length ratio of the high-Z and low-Z segments. It is found that an optimal length ratio can be obtained for each high-Z to low-Z impedance ratio to maximize the upper rejection bandwidth. A tapped-line input/output structure is exploited to create two extra transmission zeros in the stopband. The singly loaded $Q(Q_{si})$ of a tapped SIR is derived. With the aid of Q_{si}, the two zeros can be independently tuned over a wide frequency range. When the positions of the two zeros are purposely located at the two leading higher order harmonics, the upper rejection band can be greatly extended. Chebyshev bandpass filters with spurious resonances up to $4.4f_o$, $6.5f_o$, and $8.2f_o$ are fabricated and measured to demonstrate the idea.**

***Index Terms*—Microstrip, microwave filter, spurious response, stepped impedance resonator (SIR), transmission zero.**

I. Introduction

In THE RF front-end of a modern communication system, bandpass filters with wide stopband and high selectivity are usually required to enhance the overall system performance. Over the past 30 years, the parallel-coupled microstrip filter has been one of the most commonly used filters due to its planar structure, ease of synthesis method, and low cost [1]. It is known that the traditional parallel-coupled microstrip filters suffer from the spurious responses at $2f_o$, twice the passband frequency, which may seriously degrade the attenuation level in the stopband and passband response symmetry [2]. It results from the deviation between the even- and odd-mode phase velocities of each coupled section in the filter. As a result, the width of the upper stopband is less than f_o and this could limit the applicability of the filter. Many methods [3], [4] have been proposed to overcome this problem.

The stepped impedance resonators (SIRs) have been found advantageous in designing microstrip bandpass filters [5]–[9] with good stopband performance. One of the key features of an SIR is that its resonant frequencies can be tuned by adjusting its structural parameters, such as the impedance ratio of the high-Z and low-Z segments. As a result, the first spurious harmonic can be much higher than $2f_o$. For example, the design in [7] completely suppresses the $2f_o$ resonance with an inductive effect, and the first parasitic response is observed at frequencies close to $3f_o$. A combination of different SIR structures can also be adopted for a bandpass filter with wide stopband [8], [9]. Nonconventional SIRs [8] can be used to construct high-performance bandpass filters with the control of spurious responses outside of a selected bandwidth over a very large frequency range. In [10], low-pass structures are integrated within bandpass topologies. By adjusting low-pass filter cutoff frequencies, harmonic resonances of distributed bandpass filters are attenuated. A multilayer solution is proposed to overcome some design limitations, such as realizable characteristic impedance values.

Filters with a tapped-line input can save space, as well as cost, since the first and last sections of the filter are eliminated [11]. A further benefit is that two independent extra transmission zeros in the stopband can be easily created without requiring complex coupling between resonators [12]–[14]. It means that, without altering the passband response, we can apply tapped couplings to both the first and last resonators to fully control the positions of the two extra zeros. This is a very useful feature for practical receivers in rejecting image frequencies and enhancing the rejection level in the stopband of a bandpass filter.

In this paper, we aim at designing a bandpass filter with a very wide stopband possessing a satisfactory rejection level. To this end, first, SIRs are used as building blocks to push the second, third, and fourth resonances to as high frequencies as possible. The filter is synthesized based on a parallel-coupled structure. With proper input and output tappings, two transmission zeros are then created and devoted to cancel the first higher order resonance so that the filter has a very wide stopband up to the second spurious resonance. Finally, the two zeros are used to suppress the first and second higher order harmonics in a one-on-one manner, so that the stopband of the filter can be extended up to the third higher order harmonic or the fourth resonant frequency of the SIR.

This paper is organized as follows. Section II analyzes the resonance characteristics of an SIR. For an SIR with given impedance ratio, Section III investigates the optimal length ratio to obtain a maximally wide stopband. Section IV addresses the tuning of the extra transmission zeros, and formulates the singly loaded $Q(Q_{si})$ of a tapped SIR. Section V gives the design procedure for an SIR filter, and Section VI presents some simulation and experimental results.

Manuscript received July 25, 2002; revised November 19, 2002. This work was supported in part by the National Science Council, Taiwan, R.O.C., under Grant NSC 90-2213-E-009-062, and by the Ministry of Education and the National Science Council Joint Program under Contract 89-E-F-A06-2-4.

The authors are with the Department of Communication Engineering, National Chiao Tung University, Hsinchu 300, Taiwan, R.O.C. (e-mail: jtkuo@cc.nctu.edu.tw).

Digital Object Identifier 10.1109/TMTT.2003.810138

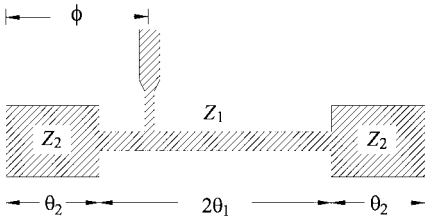

Fig. 1. Structure of an SIR with tapped input.

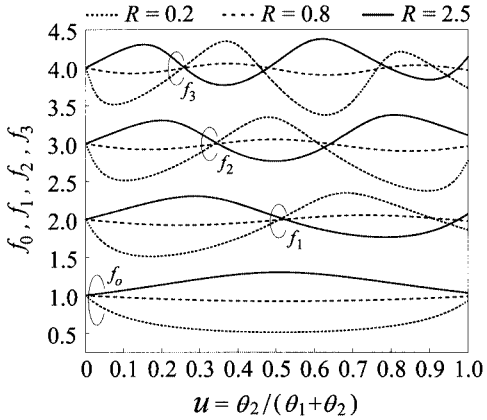

Fig. 2. Normalized resonant frequencies of an SIR.

II. Resonant Properties of an SIR

Shown in Fig. 1 is the structure for a typical SIR, of which an infinite number of resonant frequencies exist. Each resonance has either a symmetric (even-mode) or an antisymmetric (odd-mode) voltage distribution on the resonator. The fundamental resonance occurs in the odd mode, and the first higher order resonance in an even mode, and so forth. The conditions for determining the resonance frequencies of an SIR are given as [5]

$$\tan\theta_1 = R\cot\theta_2 \text{ (odd-mode)} \tag{1}$$

$$\cot\theta_1 = -R\cot\theta_2 \text{ (even-mode)} \tag{2}$$

where R is the impedance ratio of the SIR defined as

$$R = \frac{Z_2}{Z_1}. \tag{3}$$

When $R = 1$, $\theta_1 + \theta_2 = \pi/2$ at f_o. It can be seen from (1) and (2) that the resonant frequencies of an SIR can be tuned by changing the value of R and the lengths of the high-Z and low-Z segments. A simple root-searching program can be employed to calculate the resonant frequencies of the structure. For a microstrip SIR on a dielectric substrate with $\varepsilon_r = 2.2$ and high-$Z = 105\ \Omega$, Fig. 2 plots the resonant frequencies f_k against $u = \theta_2/(\theta_1+\theta_2)$ for the fundamental, first, second, and third higher order modes for $R = 0.2$, 0.8, and 2.5. These resonant frequencies have been normalized with respect to the fundamental frequency of a uniform impedance resonator (UIR), i.e., $Z_1 = Z_2$. It can be observed that, if $R \neq 1$, the f_k plot has $k+1$ extreme values as u is varied from 0 to 1. All these extreme frequencies occur at different values of u. For example,

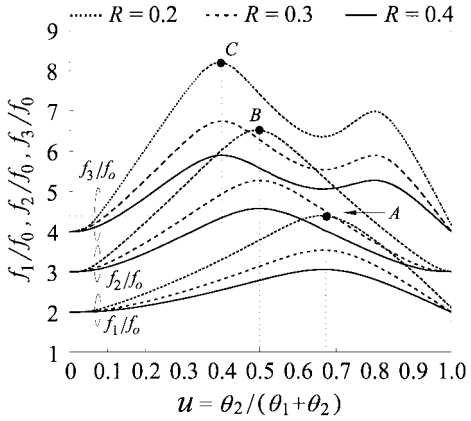

Fig. 3. Ratios of the three leading higher order resonant frequencies to the fundamental frequency of an SIR for $R = 0.2, 0.3$, and 0.4.

when $R = 0.2$, the fundamental resonant frequency has a minimum at $u \approx 0.5$, and the second higher order resonance has two minimal frequencies at $u \approx 0.1$ and $u \approx 0.9$ and a maximal frequency at $u \approx 0.48$.

III. Optimal Design for Wide Stopband

Since the object of our design is to look for a bandpass with a stopband as wide as possible, the space between each of the higher order resonant frequencies and the fundamental one is of the paramount concern. Thus, Fig. 3 plots the higher order resonant frequencies normalized with respect to their associated f_o for $R = 0.2, 0.3$, and 0.4. Here, the optimal u value for obtaining a maximal f_k/f_o for each R value is clearly indicated. For example, when $R = 0.2$, u should be 0.68, 0.5, and 0.4 to locate the higher order resonant frequencies at $4.4f_o$, $6.5f_o$, and $8.2f_o$, as indicated by points A, B, and C, respectively. It is to be noted that the smaller the values of R are, the larger the maximal f_k/f_o ratio is. In [5], several maximal f_k to f_o ratios are also plotted versus R values, but they are limited to the case of $\theta_1 = \theta_2$ or $u = 0.5$. If u can be changed freely, as indicated in Fig. 3, the maximal values of f_1/f_o and f_3/f_o can be increased significantly.

IV. Create Transmission Zeros by Tapping the I/O Resonators

The couplings between the feed lines and end resonators of a bandpass filter can be performed with gap or tapped coupling. When the latter is used, the singly loaded $Q(Q_{si})$ of a resonator should be calculated. The value of Q_{si} should be determined by the filter specification, which specifies the passband response. For a tapped resonator, the Q_{si} value is given as [5]

$$Q_{si} = R_L \frac{\omega_o}{2} \left.\frac{dB}{d\omega}\right|_{\omega_o} \tag{4}$$

where R_L is the load impedance seen by the resonator looking into the load at the tap point, ω_o is the operation frequency, and B is the total susceptance of the resonator seen by the feed line at the tap point. Thus, Q_{si} for the tapped SIR in Fig. 1 can be derived as follows.

When $0 < \phi < \theta_2$

$$\frac{Q_{si}}{R_L} = \frac{1}{2Z_2}\left\{\phi\sec^2(\phi) + \sec^2(\theta_2 - \phi) \cdot \frac{(\theta_2 - \phi)\left[R^2 + f^2(\theta_2)\right] + Rh(\theta_2)}{\left[f(\theta_2) - R\tan(\theta_2 - \phi)\right]^2}\right\} \quad (5a)$$

where

$$f(\theta_2) = \frac{R - \tan(\theta_2)\tan(2\theta_1)}{\tan(\theta_2) + R\tan(2\theta_1)} \quad (5b)$$

and

$$h(\theta_2) = \frac{\sec^2(2\theta_1)\left\{(2\theta_1)\left[\tan^2(\theta_2) + R^2\right] + R\theta_2\sec^2(\theta_2)\right\}}{\left[\tan(\theta_2) + R\tan(2\theta_1)\right]^2}. \quad (5c)$$

When $\theta_2 < \phi < \theta_1 + \theta_2$

$$\frac{Q_{si}}{R_L} = \frac{1}{2Z_1}\left[f^2(p)\,h(p) + f^2(q)\,h(q)\right] \quad (5d)$$

where

$$p = 2\theta_1 + \theta_2 - \phi \quad (5e)$$

$$q = \phi - \theta_2 \quad (5f)$$

$$f(\zeta) = \frac{\sec(\zeta)}{R - \tan(\theta_2)\tan(\zeta)} \quad (5g)$$

and

$$h(\zeta) = R\theta_2\sec^2(\theta_2) + \zeta\left[R^2 + \tan^2(\theta_2)\right]. \quad (5h)$$

One can easily validate that these results reduce to those in [5] when $\theta_1 = \theta_2$.

Assume that the right-hand-side portion of the tapped SIR in Fig. 1 is coupled with the next SIR in a filter. Based on [12] and [13], an extra transmission zero can be created via this tapped coupling. The frequency of the zero is determined by treating the cascaded nonuniform line sections to the left-hand side of the tap point as a quarter-wave open stub so that the input impedance at the tap point is virtually short circuited.

The frequency of the transmission zero can be tunable if the tap point can be freely sliding on the I/O SIRs. However, the Q_{si} value of the SIRs cannot be changed since it has been determined by the filter specification. When the tap point is chosen for a prescribed zero frequency, based on (4), the R_L value can be altered correspondingly to keep the Q_{si} value unchanged. If the required R_L does not equal 50 Ω, a quarter-wave transformer can be employed to perform the impedance transformation. Fig. 4 plots the simulation responses with tunable transmission zeros for a third-order SIR filter with $f_o = 2.45$ GHz and fractional bandwidth $\Delta = 10\%$. The high-Z segment has $Z_1 = 105\ \Omega$, and $R = 0.7$. Herein, the fabricated and simulated circuits use the RT/Duroid 5880 substrate with $\varepsilon_r = 2.2$ and thickness $= 0.508$ mm, and the circuit simulator is IE3D.[1]

[1]Zeland Software Inc., Fremont, CA, Jan. 1997.

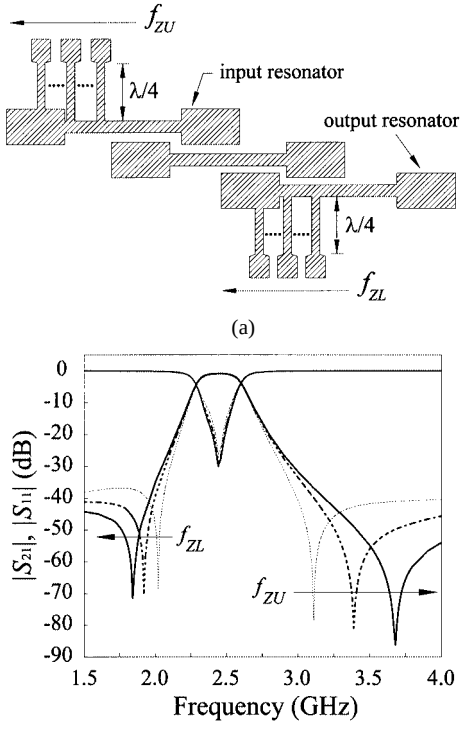

Fig. 4. Creating tunable transmission zeros by tapping the input and output resonators. (a) Circuit scheme. (b) Simulated responses. Related parameters are: $f_o = 2.45$ GHz, $\Delta = 10\%$, $R = 0.7$, and $\theta_1 = \theta_2$. The $\phi/(\theta_1 + \theta_2)$ values for generating the decreasing f_{ZL} are 1.213, 1.273, and 1.322, and those for the increasing f_{ZU} are 0.787, 0.727, and 0.678.

Fig. 4(a) shows the slide of feed lines, together with an impedance transformer, on the input and output resonators. The tap position ϕ is defined in Fig. 1, and the corresponding changes of the zeros in the lower (f_{ZL}) and upper (f_{ZU}) stopbands are shown in Fig. 4(b). It is to be noted that the passband responses are unchanged when the locations of the zeros are changed. It is obvious that the two zeros created by the input and output tappings can be freely chosen to locate in either only one or both of the stopbands. This has been validated with measurements [15].

V. Filter Design Procedure

In designing a parallel-coupled bandpass filter with SIRs, the interstage couplings required for prescribed filter function are given as [16]

$$K_{j,j+1}\big|_{j=1\text{ to }N-1} = \frac{\Delta}{\sqrt{g_j g_{j+1}}} \quad (6)$$

where g_j's are the element values of the low-pass filter prototype, Δ is the fractional bandwidth, and N is the order of the filter. This coupling coefficient is used to determine the spacing between two adjacent SIRs. In obtaining the coupling coefficient of an isolated pair of SIRs by a circuit simulator, each SIR is spaced with a gap to the feeding line. The coupling coefficient is calculated as

$$K_{j,j+1} = \frac{f_b^2 - f_a^2}{f_b^2 + f_a^2} \quad (7)$$

TABLE I
SPECIFICATIONS AND DIMENSIONS OF THE FOUR EXPERIMENTAL FILTERS

Filter	N	Δ	K_{12}	K_{23}	K_{34}	K_{45}	Q_{si}	R	W_1 (mm)	W_2 (mm)	L_1 (mm)	L_2 (mm)	S_{12} (mm)	S_{23} (mm)
Fig.5	3	10%	0.092	0.092	-	-	10.32	0.4	0.4	2.01	9.060	17.592	0.510	-
Fig.6	3	6%	0.055	0.055	-	-	17.20	0.2	0.4	5	6.350	12.330	0.200	-
Fig.8	5	10%	0.080	0.061	0.061	0.080	11.47	0.2	0.4	5	9.400	8.855	0.226	0.370
Fig.9	5	10%	0.080	0.061	0.061	0.080	11.47	0.2	0.4	5	11.500	7.199	0.376	0.526

where f_a and f_b are the resonant frequencies in the transmission response. Both conductors and dielectric substrate are assumed loss free to have f_a and f_b with good accuracy. For the first and last SIRs, the external Q's are given as [16]

$$Q_{\text{ext}} = \frac{g_o g_1}{\Delta} \tag{8a}$$

$$Q_{\text{ext}} = \frac{g_N g_{N+1}}{\Delta}. \tag{8b}$$

If the SIRs are considered lossless, Q_{si} in (5) should be in accordance with these external Q's. In other words, given the load impedance, the tapped positions of feed lines at the end resonators should be determined by the external Q's in (8).

VI. SIMULATION AND MEASUREMENT

From Fig. 3, the value of R should be chosen as low as possible for constructing an SIR filter with a wide stopband. A microstrip line, however, has a realizable impedance value with upper as well as lower limits. These limits depend on dielectric constant and thickness of the substrate, resolution of layout in fabrication process, and size of the circuit. In this study, the high-Z segment is chosen to have a linewidth of 0.4 mm, which has a characteristic impedance $Z_1 = 105\ \Omega$ and, more importantly, a tolerable metallic loss.

In the following experimental examples, the values of R are chosen to be 0.2 and 0.4. The corresponding linewidths for Z_2-segments are given in Table I. The unloaded-Q can be degraded in accordance with small R. By invoking the full-wave simulator, the unloaded $Q(Q_u)$ of the SIRs with $R = 0.2$ and 0.4 are found to be 170 and 172, respectively. The substrate parameters with regard to circuit loss, i.e., $\sigma = 5.8 \times 10^7$ S/m and $\tan\delta = 5 \times 10^{-4}$ are included in the simulation. For all the particular cases shown below, the calculated external $Q(Q_{\text{ext}})$ values for the input and output resonators are no more than 17.2, which is much less than the Q_u values of the resonators. Thus, in addition to the conductor and dielectric losses, the radiation effect, which is possibly further enhanced by the impedance junctions of the SIR, can be neglected. These loss factors are not taken into account for the ease of design.

Several SIR filters are designed and fabricated to validate the above-described findings. The circuit parameters and detailed dimensions of each filter are listed in Table I, where W_i and L_i represent the linewidth and length of the Z_i-segment of a single SIR, respectively, and $S_{j,j+1}$ is the spacing between the jth and $(j+1)$th SIRs.

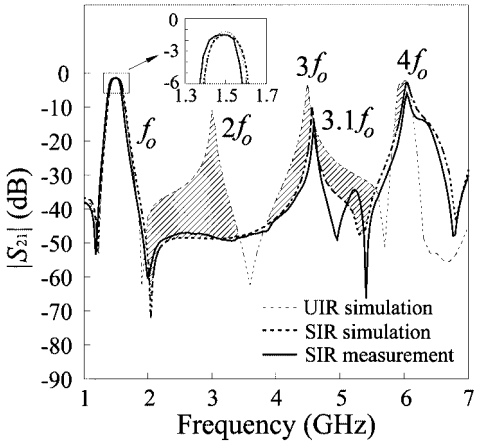

Fig. 5. Simulated and measured responses for an SIR filter. $f_o = 1.5$ GHz, $N = 3$, $R = 0.4$, $\Delta = 10\%$, and passband ripple = 0.1 dB. Simulated result for a UIR filter with identical specification is also plotted for comparison.

Fig. 5 shows simulated results for a third-order Chebyshev filter with a 0.1-dB ripple level. The filter has $f_o = 1.5$ GHz, $\Delta = 10\%$, and $R = 0.4$. The simulation $|S_{21}|$ response of a UIR filter with identical passband specification is also plotted for comparison. The SIR filter has the first spurious passband at $3.1f_o$, as predicted in Fig. 3, which is much higher than the second spurious response of the UIR filter. Furthermore, this spurious response shows a bandwidth much smaller than the second spurious response of the UIR filter. In Fig. 5, a zoomed area is used to show in detail the fundamental passband performance of the designed bandpass filter. At the center of the passband, the insertion loss of the UIR filter is 0.1 dB better than that of the SIR filter. The experiment and simulation results have a good agreement.

The filter shown in Fig. 5 is redesigned with $\Delta = 6\%$ and $R = 0.2$, and the results are shown in Fig. 6(a). Again, the $|S_{21}|$ response for a UIR filter is also plotted for comparison. The first spurious response for the SIR filter is pushed to $4.4f_o$, as well as predicted in Fig. 3. It is interesting to note that the shadow area in the plot demonstrates the improvement of stopband rejection by the SIRs. As shown in the zoomed area, at the center of passband, the insertion loss of the UIR filter is 0.7 dB better than that of the SIR filter. Fig. 6(b) presents the photograph of the fabricated circuit.

It is worth mentioning that the attenuation level at frequencies around $2f_o$ of the filter in Fig. 6(a) is better than that of Fig. 5 by 15–25 dB. In our numerical experiments, it is found

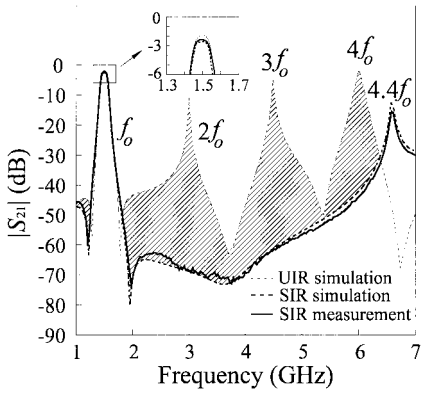

(a)

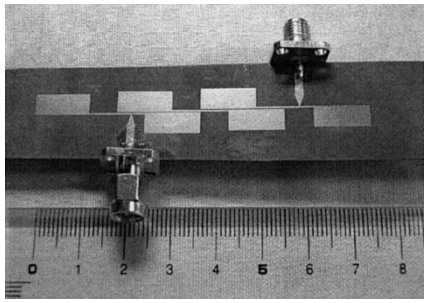

(b)

Fig. 6. (a) Simulated and measured responses for an SIR filter. $f_o = 1.5$ GHz, $N = 3$, $R = 0.2$, $\Delta = 6\%$, and passband ripple = 0.1 dB. Simulated result for a UIR filter with identical specification is also plotted for comparison. (b) Photograph of the fabricated circuit.

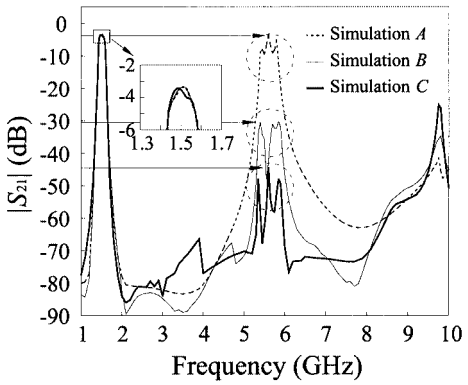

Fig. 7. Simulation responses for an SIR filter with tap-controlled transmission zeros. For case A, the tap points are determined by $R_L = 50\ \Omega$. For case B, one of the two zeros is located at the first spurious resonance $(3.76f_o)$. For case C, both zeros are at the first spurious resonance $(3.76f_o)$. $f_o = 1.5$ GHz, $N = 5$, $R = 0.2$, $\Delta = 10\%$, and passband ripple = 0.1 dB.

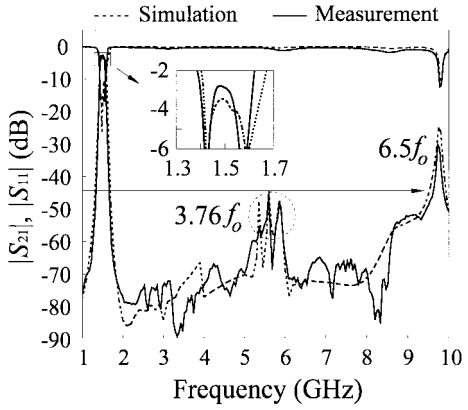

Fig. 8. Simulation and measurement responses for case C of Fig. 7.

that the attenuation level in the upper stopband also depends on the bandwidth of the filter. The choice of the R value, however, seems to dominate the attenuation level of the filter at $2f_o$. This finding leads us to use an SIR with a small R for designing filters of wide stopband with satisfactory rejection levels in the upper stopband.

In both Figs. 5 and 6(a), the two transmission zeros on both sides of the passband are created by tapping the input and output resonators without any tuning. It means that the tap point is determined by the Q_{si} value with $R_L = 50\,\Omega$, and there is no need using any quarter-wave transformer.

In Fig. 3, the peak value of f_2/f_o for $R = 0.2$ is 6.5. To reach this goal, we can use the two extra zeros, created by tapping the input and output resonators, to cancel the first spurious resonance at $3.76f_o$. The effectiveness of suppressing the spurious resonance using only one zero is, of course, different from that using two. This is investigated in Fig. 7 with a fifth-order bandpass filter, whose $\Delta = 10\%$ and $f_o = 1.5$ GHz. It is to be noted that $u = 0.5$ should be used to have $f_2/f_o = 6.5$.

There are three plots shown in Fig. 7. For simulation A, the tap points are determined by $R_L = 50\ \Omega$, and no impedance transformer is required. For simulation B, one of the two zeros is located at the first spurious resonance ($3.76f_o$ or 5.6 GHz); and for simulation C, both zeros are located at the first spurious resonance. Case A has a peak spurious $|S_{21}|$ value of higher than -5 dB at $3.76f_o$, while cases B and C have approximately -30 and -45 dB, respectively. It is interesting to note that the $|S_{21}|$ for plot A at f_o is below -40 dB. The reason is that $6.5f_o$ is a higher order zero created by tapping at one of the end resonators. This issue is outside of the scope of this paper, and will be discussed in another form.

Fig. 8 compares the simulation and measured responses for case C of Fig. 7. It can be observed that both responses have a good agreement. Their worst rejection levels in the entire upper stopband are -45 dB before the spurious response goes up.

From the results shown in Fig. 7, it is possible to exploit the two transmission zeros to cancel the two leading spurious resonances in the upper stopband with a tradeoff of the attenuation level. If this is done for the case of $R = 0.2$, the stopband can be further extended to $8.2f_o$, the third spurious harmonic, as predicted in Fig. 3. To this end, we have to choose $u = 0.2$ and move the tapping to the positions that creates transmission zeros whose frequencies equal the first and second spurious resonances of the SIR at $3.3f_o$ and $6.0f_o$, respectively. Fig. 9(a) plots the simulated and measured responses of the bandpass filter. A minimal rejection level of -30 dB is obtained in the stopband before the third spurious response at $8.2f_o$ rises. Fig. 9(b) shows the photograph of the filter.

It is to be noted that, in our experience of measuring the responses of filters of Figs. 6, 8 and 9, the results in the stopband can be quite sensitive to the flatness of the circuit board. Since the RT/Duroid 5880 substrate is a soft board, a metallic carrier is suggested to support the circuit during the measurement.

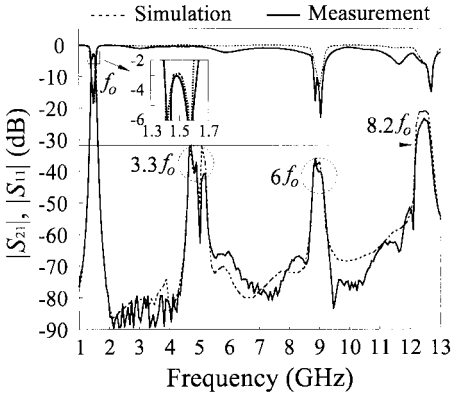

(a)

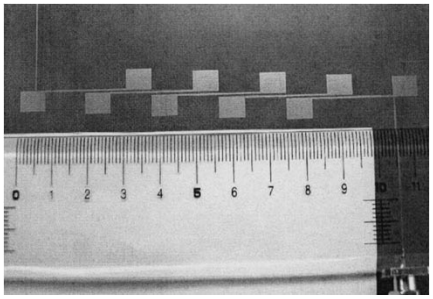

(b)

Fig. 9. (a) Simulation and measured responses of the fabricated filter. (b) Photograph of the circuit. The passband specification of the filter is identical to that of Fig. 8.

VII. Conclusion

Given a characteristic impedance ratio of the high-Z and low-Z segments, an SIR is shown to have a maximally wide stopband for certain length ratios of the segments. Filters with SIRs of lower impedance ratios are found to have higher spurious resonant frequencies and better rejection levels at $2f_o$, twice the passband frequency. The singly loaded $Q(Q_{si})$ for a tapped SIR is derived. It is shown that proper tappings at both the input and output resonators can create two independent tunable transmission zeros in the stopband, which can be used to improve the attenuation and selectivity of the filters. Bandpass filters with stopbands up to $4.4f_o$, $6.5f_o$, and $8.2f_o$ are designed and fabricated. A very good agreement between the simulation and measurement is obtained.

References

[1] D. M. Pozar, *Microwave Engineering*, 2nd ed. New York: Wiley, 1998, ch. 8.

[2] C.-Y. Chang and T. Itoh, "A modified parallel-coupled filter structure that improves the upper stopband rejection and response symmetry," *IEEE Trans. Microwave Theory Tech*, vol. 39, pp. 310–314, Feb. 1991.

[3] A. Riddle, "High performance parallel-coupled microstrip filters," in *IEEE MTT-S Int. Microwave Symp. Dig.*, 1988, pp. 427–430.

[4] I. J. Bahl, "Capacitively compensated high performance parallel-coupled microstrip filters," in *IEEE MTT-S Int. Microwave Symp. Dig.*, 1989, pp. 679–682.

[5] M. Makimoto and S. Yamashita, "Bandpass filters using parallel-coupled stripline stepped impedance resonators," *IEEE Trans. Microwave Theory Tech.*, vol. MTT-28, pp. 1413–1417, Dec. 1980.

[6] S.-Y. Lee and C.-M. Tsai, "New cross-coupled filter design using improved hairpin resonator," *IEEE Trans. Microwave Theory Tech.*, vol. 48, pp. 2482–2490, Dec. 2000.

[7] L. Zhu and K. Wu, "Accurate circuit model of interdigital capacitor and its application to design of new quasi-lumped miniaturized filters with suppression of harmonic resonance," *IEEE Trans. Microwave Theory Tech.*, vol. 48, pp. 347–356, Mar. 2000.

[8] S. Denis, C. Person, S. Toutain, S. Vigneron, and B. Theron, "Improvement of global performances of band-pass filters using nonconventional stepped impedance resonators," in *28th Eur. Microwave Conf. Dig.*, 1998, pp. 323–328.

[9] M. Makimoto and S. Yamashita, *Microwave Resonators and Filters for Wireless Communication—Theory and Design*. Berlin, Germany: Springer, 2001, pp. 79–83.

[10] C. Quendo, E. Rius, C. Person, and M. Ney, "Integration of optimized low-pass filters in a bandpass filter for out-of-band improvement," *IEEE Trans. Microwave Theory Tech.*, vol. 49, pp. 2376–2383, Dec. 2001.

[11] J. S. Wong, "Microstrip tapped-line filter design," *IEEE Trans. Microwave Theory Tech.*, vol. MTT-27, pp. 44–50, Jan. 1979.

[12] M. Matsuo, H. Yabuki, and M. Makimoto, "The design of a half-wavelength resonator BPF with attenuation poles at desired frequencies," in *IEEE MTT-S Int. Microwave Symp. Dig.*, 2000, pp. 1181–1184.

[13] K. Wada and I. Awai, "Heuristic models of half-wavelength resonator bandpass filter with attenuation poles," *Electron. Lett.*, vol. 35, no. 5, pp. 401–402, Mar. 1999.

[14] K. Wada and O. Hashimoto, "Fundamentals of open-ended resonators and their application to microwave filters," *IEICE Trans. Electron.*, vol. E83-C, no. 11, pp. 1763–1775, Nov. 2000.

[15] J.-T. Kuo and E. Shih, "Stepped impedance resonator bandpass filters with tunable transmission zeros and its application to wide stopband design," in *IEEE MTT-S Int. Microwave Symp. Dig.*, 2002, pp. 1613–1616.

[16] G. L. Matthaei, L. Young, and E. M. T. Jones, *Microwave Filters, Impedance-Matching Network, and Coupling Structures*. Norwood, MA: Artech House, 1980.

Jen-Tsai Kuo (S'88–M'92) received the Ph.D. degree from the Institute of Electronics, National Chiao Tung University (NCTU), Hsinchu, Taiwan, R.O.C., in 1992.

Since 1984, he has been with the Department of Communication Engineering, NCTU, as a Lecturer in both the Microwave and Communication Electronics Laboratories. He became a Professor in 2000. From 1995 to 1996, he was a Visiting Scholar with the University of California at Los Angeles. His research interests include the analysis and design of microwave circuits, high-speed interconnects and packages, field-theoretical studies of guided waves, and numerical techniques in electromagnetics.

Eric Shih was born in Taoyuan, Taiwan, R.O.C., on April 12, 1976. He received the B.S. degree in engineering and system science from the National Tsing Hua University (NTHU), Hsinchu, Taiwan, R.O.C., in 1998, and is currently working toward the Ph.D. degree in communication engineering at the National Chiao Tung University (NCTU), Hsinchu, Taiwan, R.O.C.

His research interests include the design of microwave planar filters and associated RF modules for microwave and millimeter-wave applications.